

## Article

# Usefulness Evaluation for Nonlocal Means Algorithm in Low-Dose Computed Tomography with Various Iterative Reconstruction Intensities and Kernels: A Pilot Study

Chaehyeon Song <sup>1,†</sup>, Yubin Jin <sup>1,†</sup>, Jina Shim <sup>2</sup>, Seong-Hyeon Kang <sup>3</sup> and Youngjin Lee <sup>1,\*</sup>

<sup>1</sup> Department of Radiological Science, Gachon University, 191, Hambakmoero, Yeonsu-gu, Incheon 21936, Republic of Korea; cogus1205@gachon.ac.kr (C.S.); yubin5623@gachon.ac.kr (Y.J.)

<sup>2</sup> Department of Diagnostic Radiology, Severance Hospital, 50-1, Yonsei-ro, Seodaemun-gu, Seoul 03722, Republic of Korea; eoeornfl@yuhs.ac

<sup>3</sup> Department of Biomedical Engineering, Eulji University, 553, Sanseong-daero, Sujeong-gu, Seongnam-si 13135, Republic of Korea; tjdgus7345@eulji.ac.kr

\* Correspondence: yj20@gachon.ac.kr

† These authors contributed equally to this work.

**Abstract:** The aim of this study was to evaluate the application feasibility of the nonlocal means (NLM) noise reduction algorithm in low-dose computed tomography (CT) images using an advanced modeled iterative reconstruction (ADMIRE) iterative reconstruction technique-based tin filter with various applied parameters. Low-dose CT images were based on high pitch and tin filters and acquired using slices of the aortic arch, the four chambers of the heart, and the end of the heart. Intensities A2 and A3 as well as kernels B40 and B59 were used as the parameters for the ADMIRE technique. The NLM denoising algorithm was modeled based on the principle of weighting between pixels; the contrast-to-noise ratio (CNR), edge rise distance (ERD), and blind/referenceless image spatial quality evaluator (BRISQUE) were used as image quality evaluation parameters. The CNR result was the highest, with an average of 43.51 in three slices when the proposed NLM denoising algorithm was applied to CT images acquired using the ADMIRE intensity 2 and B59 kernel. The ERD results were similar to those obtained using the ADMIRE intensity 2 and B59 kernel in the CT image acquired using the proposed method. In addition, BRISQUE, which can evaluate the overall image quality, showed a similar trend to the ERD results. In conclusion, the NLM noise reduction algorithm is expected to maximize image quality by preserving efficient edge information while improving noise characteristics in low-dose CT examinations.

**Keywords:** non-local means noise reduction algorithm; low-dose CT; iterative reconstruction; quantitative evaluation of image quality



**Citation:** Song, C.; Jin, Y.; Shim, J.; Kang, S.-H.; Lee, Y. Usefulness Evaluation for Nonlocal Means Algorithm in Low-Dose Computed Tomography with Various Iterative Reconstruction Intensities and Kernels: A Pilot Study. *Appl. Sci.* **2024**, *14*, 3392. <https://doi.org/10.3390/app14083392>

Academic Editor: Yang Long

Received: 1 February 2024

Revised: 7 April 2024

Accepted: 13 April 2024

Published: 17 April 2024



**Copyright:** © 2024 by the authors. Licensee MDPI, Basel, Switzerland. This article is an open access article distributed under the terms and conditions of the Creative Commons Attribution (CC BY) license (<https://creativecommons.org/licenses/by/4.0/>).

## 1. Introduction

Computed tomography (CT), which was developed by Hounsfield in 1972, uses projection data obtained by rotating opposite X-ray tubes and detectors to express the anatomical structure of the internal cross-section of the human body as an image. CT, which has the advantages of obtaining high-resolution images, is steadily increasing in the field of diagnostic medical imaging [1–3]. However, studies have reported that CT scans have the disadvantage of having a higher exposure dose for patients than other diagnostic techniques, thereby contributing to an increase in the incidence of cancer [4,5]. As the number of CT scans per year increases, the incidence rate ratio increases proportionally [6]; studies have shown that 1.5–2.0% of all cancer occurrences are estimated to be due to CT use [7]. Therefore, there is an increasing need for low-dose CT to reduce radiation exposure in patients.

However, during low-dose CT tests, noise in the image inevitably increases, thus resulting in a decrease in the overall image quality and diagnostic accuracy [8]. The

methods for solving these problems can be broadly classified into three types: The first method uses an additional filter that is capable of obtaining improved image quality from the hardware of the CT system. Additional filters are also used in X-ray-based imaging systems. Although the additional filter plays a role in reducing the patient's exposure dose, the disadvantage of inevitably increasing the noise of the image due to the decrease in the number of photons detected occurs simultaneously. To overcome these shortcomings, many researchers have proposed and developed additional filters using tin instead of conventional aluminum or copper materials [9]. The use of tin filters removes low-energy regions from the X-ray spectrum, thereby reducing the radiation dose by 81% during CT scans and minimizing the noise generated as compared to conventional filters [10].

The second noise removal method involves the use of a CT image postprocessing technique. The most representative techniques are the median filter [11], which utilizes the median value of pixels, and the Wiener filter [12], which is based on the principle of minimizing the average square error between images. However, when these filters are applied to X-ray images, the disadvantages include a decrease in noise removal efficiency and in the sharpness of the border area [13]. To compensate for these shortcomings, a noise cancellation algorithm using a nonlocal means (NLM) algorithm was developed [13,14]. Algorithms using the NLM approach have been applied in various ways to improve the quality of diagnostic medical X-ray images [14,15]. Diwakar et al. proposed an NLM approach that balanced noise suppression and edge preservation level in CT images [14], and Shagnnuan et al. confirmed the applicability of NLM priorly in the iterative reconstruction process based on low-dose CT images [15].

Finally, a reconstruction technique suitable for low-dose CT imaging systems was developed. Currently, the most commonly used reconstruction technique in clinical practice is the filtered back projection (FBP). FBP is a method of converting a two-dimensional planar image of a subject acquired from various angles through filter correction, and then reversely projecting it in the acquired direction. However, this reconstruction technique has the disadvantage of significantly increasing the image noise at low doses [16]. To overcome these shortcomings, repetitive reconstruction (IR) techniques have been developed and applied in clinical trials. Unlike FBP, which processes data only once, IR techniques repeatedly process raw or reconstructed data to reduce the image noise. As a result, IR can reduce the exposure dose to patients by improving the noise level compared to FBP [16]. Among them, the Advanced Model-Based Interactive Reconstruction (ADMIRE) technique used in the Siemens CT imaging system can obtain an appropriate image quality using various parameters [17,18]. Typical parameters of ADMIRE include strength and kernel; depending on these values, the image quality of the final CT image changes.

In this study, low-dose CT images were obtained using an ADMIRE technique-based annotation filter with various parameters; the applicability of the NLM algorithm was evaluated. In this study, the noise removal efficiency and boundary preservation characteristics of the resulting images, including CT images obtained using the NLM algorithm, were measured using the contrast-to-noise ratio (CNR) and edge noise distance (ERD).

## 2. Materials and Methods

### 2.1. Low-Dose CT Scan Parameter

The study was conducted according to the guidelines of the Declaration of Helsinki and approved by the Institutional Review Board of Severance Hospital (4-2022-0356) (Seoul, Republic of Korea).

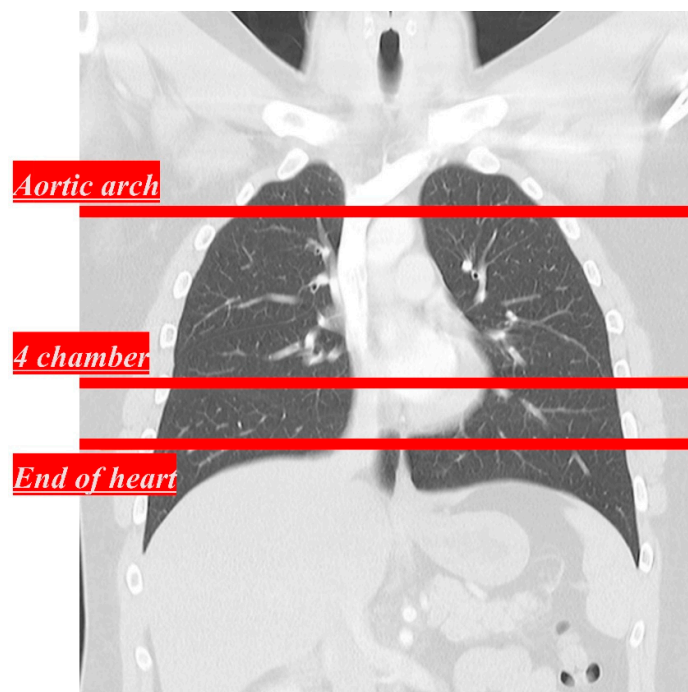
The equipment used in this study was the SOMATOM Force CT imaging system (Siemens Healthineers, Erlangen, Germany). The conditions for obtaining low-dose CT images using a tin filter are presented in Table 1. The parameters of the ADMIRE technique used strengths A2 and A3 as well as kernels B40 and B59. The strengths and kernels used in ADMIRE were the values used in general chest CT scans [19]. The four combinations of ADMIRE parameters used in this study are listed in Table 2. CT images were obtained at three positions: the aortic arch, four chambers, and the end of the heart (Figure 1).

**Table 1.** CT image acquisition parameters.

Parameter	Value
Pitch	2.5 (high pitch)
Tube voltage (kVp)	100
Average tube current (mAs)	92
Additional filter	Tin
Rotation time (s)	0.25
Slice thickness/increment (mm)	1/1
Detector collimator (mm)	192 × 0.6

**Table 2.** Four group sets for CT image acquisition.

	Group 1	Group 2	Group 3	Group 4
ADMIRE type	ADMIRE 2 + B 40	ADMIRE 3 + B 40	ADMIRE 2 + B 59	ADMIRE 2 + B 40+ NLM

**Figure 1.** Scan line for each area to acquire CT images: aortic arch, 4 chambers, and end of the heart.

## 2.2. Nonlocal Means (NLM) Noise Reduction Approach

The NLM filter takes advantage of image redundancy and obtains pixel values using the spatial information of the image. Each pixel in the NLM-filtered image identified and weighed an area similar to the surrounding area, thereby effectively eliminating noise.

$$\text{NLM}(I(i)) = \sum_{i \in N_i}^n w\{N_i, N_j\} I(j) \quad (1)$$

here,  $I(i)$  is the noise intensity of  $i$ , and  $N_i$  is the peripheral pixel of  $I$ . The weight  $w\{N_i, N_j\}$  depends on the similarity between  $i$  and  $j$  and satisfies the general value [20]. The NLM algorithm can improve image quality by solving signal distortion and blurring effects, which are problems with existing filters; the degree of distortion of pixels with noise removed from the original image is small [20].

### 2.3. Evaluation of Image Performance

In this study, the CNR and ERD were used as quantitative evaluation methods for CT image quality. The CNR is a representative factor that can be used to observe the contrast and noise levels of an image in combination; the equation is as follows:

$$\text{CNR} = \frac{|S_A - S_B|}{\sqrt{\sigma_A^2 + \sigma_B^2}} \quad (2)$$

where  $S_A$  and  $\sigma_A$  represent the average and standard deviation of the signal strength in the target area, respectively;  $S_B$  and  $\sigma_B$  represent the average and standard deviation of the signal strength in the background area, respectively. In addition, the ERD is a representative factor that can evaluate the degree to which the boundary part of the image is preserved; it can be defined as the distance between the points representing 10% and 90% of the CT number. The region of interest (ROI) for measuring the CNR and ERD is shown in the CT sample image in Figure 2.

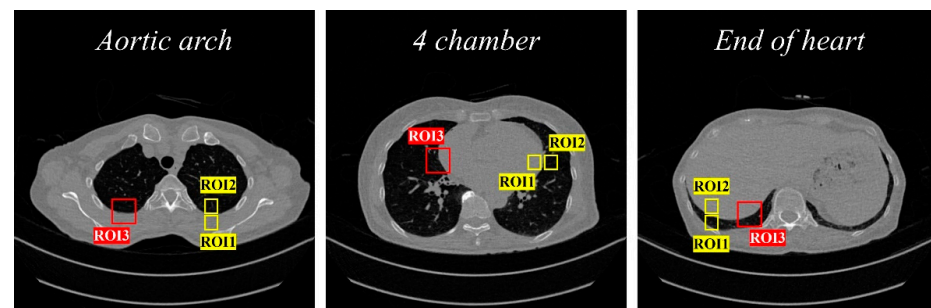


**Figure 2.** ROI area set in each CT sample image (CNR evaluation: ROI1 and ROI2, and ERD evaluation: ROI3).

In addition, to check the overall CT image quality, a blind/referenceless image spatial evaluator (BRISQUE) proposed by Mittal et al. was used as a representative factor among the non-reference-based evaluation methods [21]. The formula related to BRISQUE evaluation is as follows: the smaller the value, the more similar it is to the ideal image quality.

$$f(x; \alpha, \sigma^2) = \frac{\alpha}{2\beta\Gamma(1/\alpha)} e^{-(\frac{|x|}{\beta})^\alpha} \quad (3)$$

where  $f$  is a function based on a generalized Gaussian distribution (GGD) that can measure BRISQUE;  $\alpha$  is a model parameter;  $\sigma$  is a variance;  $\Gamma$  is a gamma function; and  $\beta$  is  $\sigma \sqrt{\frac{\Gamma(1/\alpha)}{\Gamma(3/\alpha)}}$ .

### 3. Results and Discussion

Low-dose CT images for each reconstruction parameter as obtained by selecting cross-sections of the aortic arch, four chambers of the heart, and the end of the heart are shown in Figure 3; Groups 1–4 images derived according to the parameter strengths and kernel combinations of each of the four ADMIRE techniques are also shown here. Group 4, which applied the NLM noise removal algorithm, showed the best visual quality among all the cross-sectional images. In particular, as compared with the resulting images of Group 3 using ADMIRE A2 and kernel B59, we confirmed that the noise level was significantly reduced in Group 4 using the NLM algorithm with ADMIRE A2 and kernel B59.

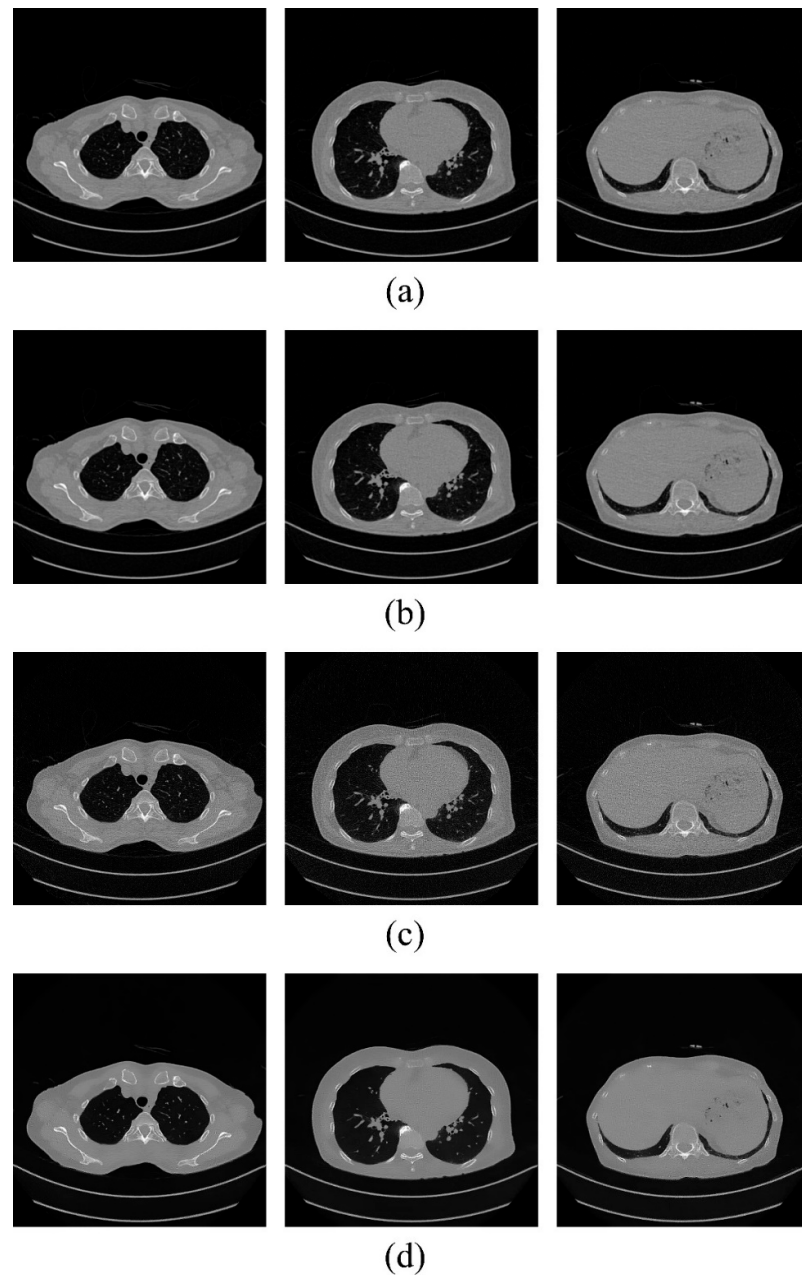


**Figure 3.** Low-dose CT images according to various ADMIRE intensities and kernel combinations: (a) AD-MIRE A with kernel B40 (Group 1); (b) ADMIRE A3 with kernel B40 (Group 2); (c) ADMIRE A2 with kernel B59 (Group 3); and (d) ADMIRE A2, kernel B59, and NLM noise reduction algorithm (Group 4).

Data on CNR, ERD, and BRISQUE values obtained in this study are shown in Table 3. The resulting data presented each quantitative indicator with respect to the group.

The resulting graphs and values of the CNR, quantitatively analyzed in the ROI set as shown in Figure 2, are presented in Figure 4. The CNR values measured in the aortic arch were approximately 56.49 in Group 1, 64.86 in Group 2, 13.79 in Group 3, and 56.25 in Group 4. In the aortic arch, the highest value was found in Group 2; high values similar to those in Group 2 were found in Group 4. Among the four chambers, Group 4 showed the most improved value at approximately 49.33, while Group 3 showed the lowest value at approximately 8.57. At the end of the heart, as in the previous images, improved results were observed in Groups 4, 2, 1, and 3; the best value of approximately 28.94 was obtained in Group 4. The highest average value was obtained in Group 4, which

applied the proposed NLM noise removal algorithm to low-dose CT images. In addition, as compared with the Group 2 images obtained based on relatively high ADMIRE intensity and low kernel, the CNR was higher in Group 4 using the NLM noise removal algorithm.

**Table 3.** Quantitative evaluation results as function of Group.

Position	Evaluation Parameter	Group 1	Group 2	Group 3	Group 4
Aortic arch	CNR	56.49	64.86	13.79	56.25
	ERD	2.77	2.71	2.61	2.53
	BRISQUE	36.87	38.58	32.45	35.10
Four chamber	CNR	28.58	32.34	8.57	49.33
	ERD	1.28	1.20	0.11	0.10
	BRISQUE	35.59	37.93	31.73	35.58
End of heart	CNR	24.85	28.40	6.45	28.94
	ERD	2.02	1.95	0.11	0.95
	BRISQUE	37.81	39.91	33.79	35.01
Average	CNR	36.64	41.87	9.60	44.84
	ERD	2.02	1.96	0.94	1.19
	BRISQUE	36.76	38.80	32.66	35.23

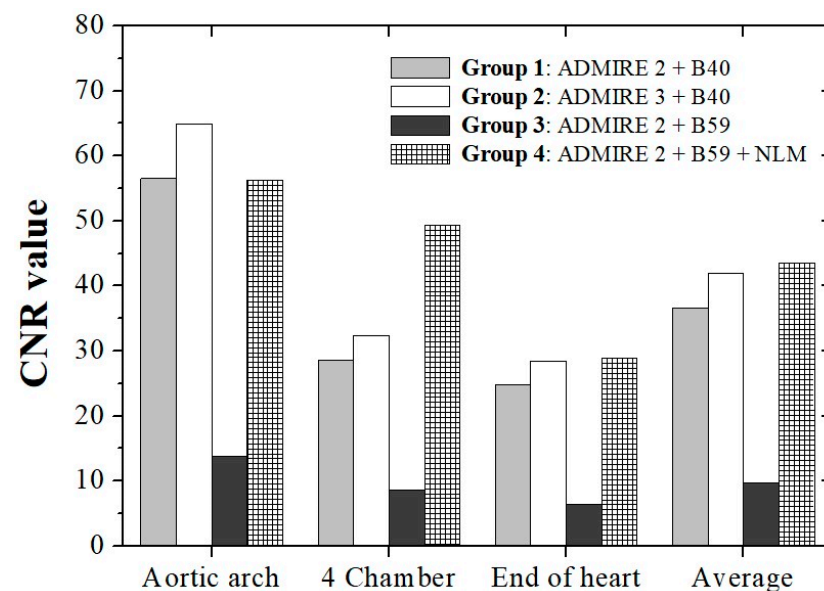


**Figure 4.** Results of contrast-to-noise ratio (CNR) for reconstructed CT images of the aortic arch, 4 chamber, and end of heart areas.

The resulting graphs and figures of the ERD, quantitatively analyzed in the ROI set as shown in Figure 2, are shown in Figure 5. The ERD values measured at the aortic arch were approximately 2.77 in Group 1, 2.71 in Group 2, 2.61 in Group 3, and 2.53 in Group 4, with Group 4 showing the best value. Among the four chambers, Group 4 showed the most improved value of approximately 0.100, while Group 1 showed the lowest value of approximately 1.28. At the end of the heart, similar to the previous images, improved values were obtained in the following order: Groups 3, 4, 2, and 1. Group 4 also showed an excellent average ERD value of approximately 1.19, which was similar to that of Group 3. As a result, the best value was obtained in Group 3 based on ADMIRE A2 and kernel B59; similar results were obtained with an average of approximately 1.19 in Group 4, which applied our proposed NLM noise removal algorithm to low-dose CT images. Additionally, in Groups 1 and 3, using the same ADMIRE A2, the ERD value of Group 3 using a high kernel significantly decreased as compared to that of Group 1 (Group 1 vs. Group 3).

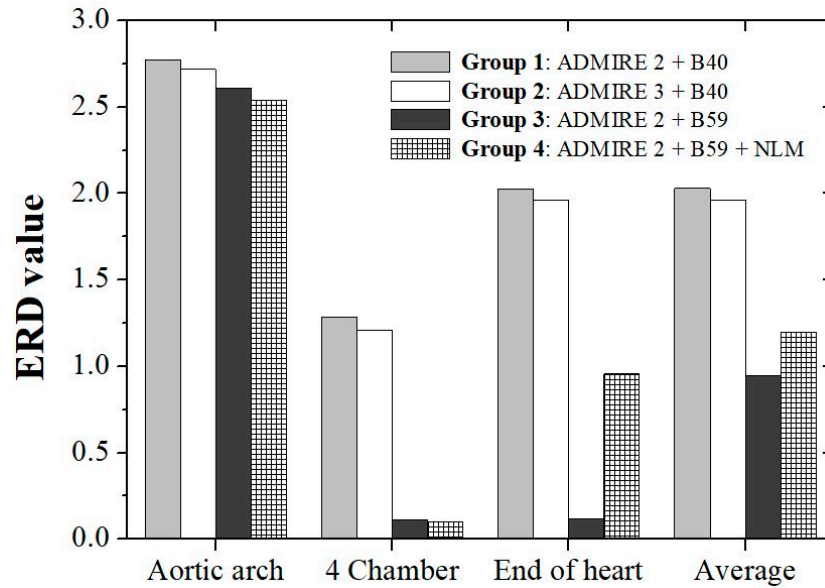


**Figure 5.** Results of edge rise distance (ERD) for reconstructed CT images of aortic arch, 4 chamber, and end of heart areas.

The results of the BRISQUE evaluation are shown in Figure 6. In the aortic arch, values of 36.87 Group 1, 38.58 Group 2, 32.45 Group 3, and 35.10, Group 4 were derived in groups 1, 2, and 3, with group 3 showing the best value. Among the four chambers, Group 3 showed the most improved value at approximately 31.73, while Group 2 showed the highest value at approximately 37.93. At the end of the heart, improved results were obtained in the following order: Groups 3, 4, 1, and 2. Similar to Group 3, Group 4 showed improved results of approximately 35.23. As a result of the BRISQUE evaluation, there was variation depending on the slice; the best value was obtained in Group 3, based on ADMIRE strength A2 and kernel B59, with an average of approximately 32.66.

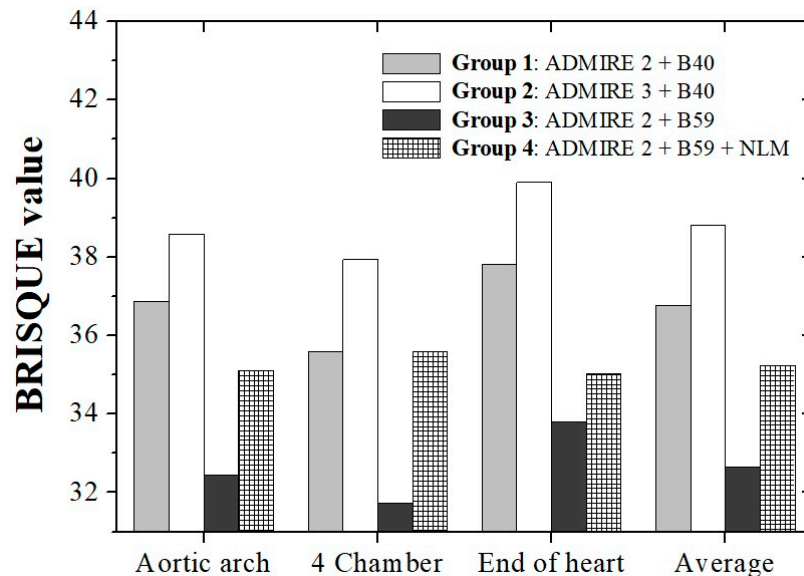


**Figure 6.** Results of blind/referenceless image spatial quality evaluator (BRISQUE) for reconstructed CT images of aortic arch, 4 chamber, and end of heart areas.

Recently, various studies have been conducted to reduce excessive radiation doses generated during the acquisition of computed tomography (CT) images. Among these, the application of additional filters is considered a hardware method. The additional filter reduces the radiation dose by removing unnecessary X-ray wavelengths reaching

the patient. Tin filters have the advantage of being able to further reduce noise compared to other additional filters, such as aluminum or copper filters that were previously used. However, tin filters cannot completely solve the noise problem because the process of removing scattered rays involves a decrease in the number of photons [9]. To solve this problem, additional technologies, including annotation filters, must be applied.

For this purpose, a software approach using image-processing techniques can be considered. Among the image-processing techniques, ADMIRE is one of the techniques applied clinically; it can improve the signal-to-noise ratio (SNR) by repeatedly processing data during low-dose CT imaging. As a feature of ADMIRE, noise removal performance improves when the intensity is increased. However, because reconstruction takes a long time, an appropriate intensity must be set according to the purpose of the CT examination. In addition, the higher the kernel, another CT parameter, is set, the lower is the smoothing strength; this reduces the degree of noise removal but has the advantage of minimizing damage to the boundary information. However, to remove a large amount of generated noise, the kernel value must be set to a low value. A low kernel value increases smoothing strength and damages boundary information. Therefore, the application of additional software that can effectively remove noise while preserving boundary information is required.

The NLM algorithm is a CT image post-processing technique that removes noise by reflecting the distance-weighted similarity of the image. When applying existing algorithms, the problems of low noise removal efficiency and low sharpness of the boundary area can be solved [13,14]. Therefore, in this study, we propose a method of additionally applying the NLM noise removal algorithm from the proposed ADMIRE and Kernel techniques to improve the noise characteristics that occur during low-dose CT examinations using annotation filters to reduce the patient's radiation dose.

As a result of the quantitative evaluation, the highest CNR was obtained in Group 4, with an average of approximately 43.51. In addition, it was measured to be approximately 4.66 times higher in Group 4 than in Group 3, based on a relatively high ADMIRE intensity and low kernel. The ERD evaluation resulted in the best value for Group 3, with an average of approximately 0.94. Group 4, which applied our proposed NLM noise removal algorithm to low-dose CT images, obtained results similar to those of Group 3, with an average of approximately 1.19. Additionally, as compared with Groups 1 and 2, Group 4 was approximately 1.69 and 1.63 times higher, respectively. This proved that the proposed NLM noise removal algorithm can effectively preserve image-edge information when reconstructing CT images. The BRISQUE evaluation yielded similar values in Groups 3 and 4, with averages of approximately 32.66 and 35.23, respectively. The noise level was reduced in the low-dose CT images obtained by increasing the intensity of ADMIRE using the same kernel (Group 1 vs. Group 2). In addition, the overall image quality was improved by reducing information loss at the border in low-dose CT images obtained using a high kernel based on the same ADMIRE intensity (Group 1 vs. Group 3). When comparing Group 3 with Groups 1 and 2, it was confirmed that Group 3 improved the image quality and maintained the edge signal of the image well; however, the noise removal efficiency was low. When comparing Group 4 with the NLM filter applied in Group 3 and in Groups 1 and 2, it was confirmed that in Group 4, as in Group 3, the signal at the edge of the image was well preserved; noise was removed more effectively. Therefore, by applying the NLM filter to Group 3, which had a low noise removal efficiency, it was confirmed that superior image quality was obtained as compared to that of Groups 1 and 2, and that edge information could be well preserved. This proves that the proposed NLM noise removal algorithm can effectively preserve the edge information of the resulting image while improving the temporal resolution measured during CT image reconstruction.

Overall, the CNR evaluation results show that the application of the NLM algorithm to low-dose CT images with a low ADMIRE and high kernel settings can solve the noise problem while maintaining an excellent temporal resolution. Additionally, ERD and BRISQUE have demonstrated that they can reduce the loss of edge information that occurs

during the NLM algorithm-based smoothing process. The proposed method can improve the quality of CT images under low-dose conditions with excellent performance because it can produce excellent image quality with excellent temporal resolution. In particular, if applied in conjunction with a tin filter that can effectively remove the radiation dose, it is expected to effectively reduce radiation exposure to patients and radiologists.

A limitation of this study is that the usefulness of the proposed noise reduction algorithm was evaluated using only one CT image. Based on the research results of this pilot concept, we plan to improve reliability by conducting statistical analysis and calculating absolute error values using CT image data by applying various ADMIRE reconstruction methods and the NLM algorithm in the future. Based on the CT image reconstruction parameters used by Solomon et al., we will further analyze the efficiency of the NLM algorithm according to each condition in the future [19]. In addition, we plan to conduct additional research on the correlation between quantitative CT image quality evaluation results and qualitative evaluation indicators using a receiver operating characteristic curve or Likert scale.

#### 4. Conclusions

This study aims to evaluate the applicability of the NLM noise removal algorithm to low-dose CT images using an annotation filter based on the ADMIRE iterative reconstruction technique by applying various parameters. For quantitative evaluation, CNR and ERD were used, and for overall image quality evaluation, BRISQUE was used to identify the aortic arch, four chambers of the heart, and end of the heart. In conclusion, the NLM noise removal algorithm is expected to maximize the image quality by simultaneously improving the noise characteristics and preserving the edge information during low-dose CT examinations.

**Author Contributions:** Conceptualization, C.S., Y.J. and Y.L.; Methodology, S.-H.K. and Y.L.; Formal analysis, J.S. and Y.L.; Funding acquisition, Y.L.; Software, S.-H.K. and Y.L.; Validation, J.S.; Writing of the original draft, C.S. and Y.J.; and Writing—review and editing, J.S., S.-H.K. and Y.L. All authors have read and agreed to the published version of the manuscript.

**Funding:** This study was supported by a grant from the National Foundation of Korea (NRF) funded by the Korean government (Grant No. NRF-2021R1F1A1061440).

**Institutional Review Board Statement:** The study was conducted according to the guidelines of the Declaration of Helsinki and approved by the Institutional Review Board of Severance Hospital (4-2022-0356).

**Informed Consent Statement:** This study was conducted retrospectively and patient consent was not obtained.

**Data Availability Statement:** The raw data supporting the conclusions of this article will be made available by the authors on request.

**Conflicts of Interest:** The authors declare no conflicts of interest.

#### References

1. Bach, P.B.; Jett, J.R.; Pastorino, U.; Tockman, M.S.; Swensen, S.J.; Begg, C.B. Computed Tomography Screening and Lung Cancer Outcomes. *JAMA* **2007**, *297*, 953–961. [[CrossRef](#)] [[PubMed](#)]
2. Choi, S.J.; Ahn, S.J.; Park, S.H.; Park, S.H.; Pak, S.Y.; Choi, J.W.; Shim, Y.S.; Jeong, Y.M.; Kim, B. Dual-source abdominopelvic computed tomography: Comparison of image quality and radiation dose of 80 kVp and 80/150 kVp with tin filter. *PLoS ONE* **2020**, *15*, e0231431. [[CrossRef](#)] [[PubMed](#)]
3. Lee, S.-J.; Park, G.; Kim, D.; Jung, S.; Song, S.; Hong, J.M.; Shin, D.H.; Lee, J.S. Clinical evaluation of a deep-learning model for automatic scoring of the Alberta stroke program early CT score on non-contrast CT. *J. NeuroInterven. Surg.* **2024**, *16*, 61–66. [[CrossRef](#)] [[PubMed](#)]
4. Cao, C.-F.; Ma, K.-L.; Shan, H.; Liu, T.-F.; Zhao, S.-Q.; Wan, Y.; Zhang, J.; Wang, H.-Q. CT Scans and Cancer Risks: A Systematic Review and Dose-response Meta-analysis. *BMC Cancer* **2022**, *22*, 1238. [[CrossRef](#)] [[PubMed](#)]

5. Mathews, J.D.; Forsythe, A.V.; Brady, Z.; Butler, M.W.; Goergen, S.K.; Byrnes, G.B.; Giles, G.G.; Wallace, A.B.; Anderson, P.R.; Guiver, T.A.; et al. Cancer risk in 680 000 people exposed to computed tomography scans in childhood or adolescence: Data linkage study of 11 million Australians. *BMJ* **2023**, *346*, f2360. [[CrossRef](#)] [[PubMed](#)]
6. Brenner, D.J.; Hall, E.J.; Phil, D. Computed Tomography—An Increasing Source of Radiation Exposure. *N. Engl. J. Med.* **2007**, *357*, 2277–2284. [[CrossRef](#)] [[PubMed](#)]
7. Ma, J.; Huang, J.; Feng, Q.; Zhang, H.; Lu, H.; Liang, Z.; Chen, W. Low-dose computed tomography image restoration using previous normal-dose scan. *Med. Phys.* **2011**, *38*, 5713–5731. [[CrossRef](#)] [[PubMed](#)]
8. Nelson III, C.A.; Gabard-Durnam, L.J. Early Adversity and Critical Periods: Neurodevelopmental Consequences of Violating the Expectable Environment. *Trends Neurosci.* **2020**, *43*, 133–143. [[CrossRef](#)] [[PubMed](#)]
9. Leyendecker, P.; Faucher, V.; Labani, A.; Noblet, V.; Lefebvre, F.; Magotteaux, P.; Ohana, M.; Roy, C. Prospective evaluation of ultra-low-dose contrast-enhanced 100-kV abdominal computed tomography with tin filter: Effect on radiation dose reduction and image quality with a third-generation dual-source CT system. *Eur. Radiol.* **2017**, *29*, 2107–2116. [[CrossRef](#)] [[PubMed](#)]
10. Ibrahim, H.; Kong, N.S.P.; Ng, T.F. Simple Adaptive Median Filter for the Removal of Impulse Noise from Highly Corrupted Images. *IEEE Trans. Consum. Electron.* **2008**, *54*, 1920–1927. [[CrossRef](#)]
11. Chen, J.; Benesty, J.; Huang, Y.; Doclo, S. New Insights into the Noise Reduction Wiener Filter. *IEEE Trans. Audio Speech Lang. Process.* **2006**, *14*, 1218–1234. [[CrossRef](#)]
12. Liu, Y.; Gui, Z.; Zhang, Q. Noise reduction for low-dose X-ray CT based on fuzzy logical in stationary wavelet domain. *Optik* **2013**, *124*, 3348–3352. [[CrossRef](#)]
13. Diwakar, M.; Kumar, P.; Singh, A.K. CT image denoising using NLM and its method noise thresholding. *Multimed. Tools Appl.* **2020**, *79*, 14449–14464. [[CrossRef](#)]
14. Diwakar, M.; Kumar, M. CT image denoising using NLM and correlation-based wavelet packet thresholding. *IET Image Process.* **2018**, *12*, 708–715. [[CrossRef](#)]
15. Shangguan, H.; Zhang, Q.; Liu, Y.; Cui, X.; Bai, Y.; Gui, Z. Low-dose CT statistical iterative reconstruction via modified MRF regularization. *Comput. Methods Programs Biomed.* **2016**, *123*, 129–141. [[CrossRef](#)] [[PubMed](#)]
16. Son, W.; Kim, M.; Hwang, J.-Y.; Kim, Y.-W.; Park, C.; Choo, K.S.; Kim, T.U.; Jang, J.Y. Comparison of a Deep Learning-Based Reconstruction Algorithm with Filtered Back Projection and Iterative Reconstruction Algorithms for Pediatric Abdominopelvic CT. *Korean J. Radiol.* **2022**, *23*, 752–762. [[CrossRef](#)] [[PubMed](#)]
17. Martini, K.; Higashigaito, K.; Barth, B.K.; Baumueller, S.; Alkadhi, H.; Frauenfelder, T. Ultralow-dose CT with tin filtration for detection of solid and sub solid pulmonary nodules: A phantom study. *Br. J. Radiol.* **2015**, *88*, 20150389. [[CrossRef](#)] [[PubMed](#)]
18. Bhujle, H.V.; Vadavadagi, B.H. NLM based magnetic resonance image denoising—A review. *Biomed. Signal Process. Control.* **2019**, *47*, 252–261. [[CrossRef](#)]
19. Solomon, J.B.; Christianson, O.; Samei, E. Quantitative comparison of noise texture across CT scanners from different manufacturers. *Med. Phys.* **2012**, *39*, 6048–6055. [[CrossRef](#)]
20. Buades, A.; Morel, J.-M. A non-local algorithm for image denoising. In Proceedings of the 2005 IEEE Computer Society Conference on Computer Vision and Pattern Recognition (CVPR'05), San Diego, CA, USA, 20–26 June 2005. [[CrossRef](#)]
21. Mittal, A.; Soundararaja, R.; Bovik, A.C. Making a “Completely Blind” Image Quality Analyzer. *IEEE Signal Process. Lett.* **2013**, *20*, 209–212. [[CrossRef](#)]

**Disclaimer/Publisher’s Note:** The statements, opinions and data contained in all publications are solely those of the individual author(s) and contributor(s) and not of MDPI and/or the editor(s). MDPI and/or the editor(s) disclaim responsibility for any injury to people or property resulting from any ideas, methods, instructions or products referred to in the content.